X-616-69-191
PREPRINT

NASA TM X-63545

THE ELECTRICAL CONDUCTIVITY AND INTERNAL TEMPERATURE OF THE MOON

NORMAN F. NESS

MAY 1969

GSFC
GODDARD SPACE FLIGHT CENTER
GREENBELT, MARYLAND

X-616-69-191

THE ELECTRICAL CONDUCTIVITY AND INTERNAL TEMPERATURE OF THE MOON*

Norman F. Ness
Laboratory for Space Sciences
NASA-Goddard Space Flight Center
Greenbelt, Maryland USA

May 1969

*Presented at XIIth COSPAR Prague 20 May 1969 as paper kll.

Extraterrestrial Physics Branch Preprint Series

Abstract

Detailed measurements of the interplanetary magnetic field in the immediate vicinity of the moon have been performed since July 1967 by Lunar Explorer 35. The magnetic field is found to be only slightly (25%) distorted with no evidence for a bow shock wave. During the interval February to July 1968, periselene (830$\pm$100 km) passed through the solar wind umbral region. A study of the propagation of discontinuities (sudden changes) in the interplanetary magnetic field through the lunar body has been completed. The induction of electrical currents in the lunar interior indicates an effective time constant for eddy current decay of less than 20 seconds. This means an electrical conductivity of less than 10^{-4} mhos/meter in the lunar interior. The electrical conductivity of silicate rocks depends mainly upon temperature. Thus limitations on possible thermal models of the moon, consistent with the electrical conductivity measurements, can be obtained. These results are compared with various models of the thermal history to obtain a class of allowed lunar interiors. The conclusion is that the moon must be a relatively young body ($1x10^9$ year old) if it possesses a homogeneous heat source composition similar to chondritic meteorites. If differentiation of radiogenic heat sources near to the surface has taken place, the moon can be old ($4x10^9$ years).

1.0 Introduction

An experimental study of the magnetic field, plasma, energetic particle and micrometeorite environment of Moon has been conducted on Lunar Explorer 35 (7). This spacecraft was placed into lunar orbit on 22 July 1967 with an orbital period of 11.53 hours. The orbital plane is inclined 169° with respect to the ecliptic plane, aposelene is 9388 ± 100 km ($5.40\ R_M$, R_M = radius of Moon = 1738 km), periselene = 2568 ± 100 km ($1.48\ R_M$) and initial aposelene-moon-sun angle = 304° East. Since injection, the spacecraft has completed more than 1400 orbits of Moon and continuously transmitted important scientific data concerning the lunar environment and interaction of the solar wind with the moon (7). Due to the heliocentric motion of the Earth-Moon system and the gravitational perturbations of Sun and Earth, the line of apsides of the orbit progresses westward approximately 1.1° per day. Thus the seasonal variation of the line of apsides is more than 360° and permits an investigation of the lunar environment at altitudes from $0.42\ R_M$ to $4.46\ R_M$ for all azimuths relative to the Moon-Sun line.

As they orbit Earth, Moon and Explorer 35 are immersed periodically in interplanetary space, the geomagnetosheath, and the geomagnetotail. When Moon is imbedded in the geomagnetic tail, it is optimumly possible to detect effects due to the magnetic properties of the lunar body. Analysis of experimental measurements (1) shows that the lunar magnetic moment is less than 10^{20} gauss cm^3 and thus the intrinsic magnetic field is less than 4 gammas on its surface. Furthermore, if the temperature of the lunar body is below the Curie point, then the magnetic susceptibility of a homogeneous Moon is less than $1.8\mu_o$.

Of special interest is the period when Moon is outside the earth's bow shock and in the interplanetary medium. The major effect of Moon on the solar wind flow is the creation of a plasma cavity with the electrons and ions impacting the lunar surface being absorbed by the lunar body (7). There is no evidence for the development of a boundary layer analogous to the earth's magnetosheath. The interplanetary magnetic field is only slightly disturbed by the presence of the moon with the principal perturbations being due to electrical currents induced in the disturbed plasma wake on the boundaries of the plasma cavity (7).

A model (8) for the magnetized solar wind flow past Moon postulates that the finite electrical conductivity of its interior will delay the motion of interplanetary magnetic field lines through the body and lead to the development of a pseudo-magnetosphere and bow shock wave. In the absence of these phenomena we conclude that the effective average electrical conductivity of the moon is less than 10^{-5} mhos/meter (5,7). However, as noted in (6), the effect of a surface layer of low conductivity can drastically alter the steady-state conditions of solar wind flow past Moon. To determine the internal electrical conductivity, it is necessary to investigate its dynamic response to discontinuities (sudden changes) in the interplanetary magnetic field (2). The decay of the eddy currents induced in the lunar interior by such transients can then be used to determine the characteristic diffusion time of the magnetic field in the interior and hence its electrical conductivity. This paper presents the first results of such a study.

2.0 Propagation of Discontinuities Past the Moon

A search of magnetic field data has been conducted, with the most important period of interest occurring when periselene (730 to 930 km from the lunar surface) passes through the lunar umbral region. During the time interval February to July 1968, over 200 orbits were investigated with the objective being to detect discontinuities propagating past the moon which were: (a) observed by Explorer 35 while in the lunar wake, and (b) which were also simultaneously observed in the interplanetary medium by the companion satellite Explorer 33. It is important to have a reference measurement of the discontinuity profile so that any variability in the intrinsic properties of the discontinuity can be separated from the effects of Moon.

A total of 6 large discontinuities, ($|\Delta\vec{B}| > 5\gamma$), satisfying the above criteria was noted and this paper discusses the largest of the events detected during this time interval. The simultaneous Explorer 33 and 35 interplanetary magnetic field data for this event are shown in Figure 1. A plot of the orbit of the spacecraft is shown in the upper left hand corner. Identified on both the trajectory plot, as well as the magnitude scale, are the characteristic umbral positive anomaly and penumbral negative and positive anomalies due to the plasma cavity.

The discontinuity under study is seen to be a sudden change in the direction of the magnetic field from essentially pointing southward relative to the ecliptic plane ($\theta = -90^{\circ}$) to northward ($\theta = +90^{\circ}$) at Explorer 35 sequence number = 249791. Note that beyond the lunar wake region the interplanetary magnetic field observed at the two widely separated satellites ($\vec{D} = 56\ R_E = 3.5\text{x}10^5$ km) is essentially identical. Within the lunar wake, the apparently large discrepancy in the azimuthal angle φ is understood as in fact a very small vector disturbance. The magnetic field is almost pointed to one of the poles of the solar ecliptic coordinate system and hence φ is not a good measure of angular deviation between the vectors measured by the two spacecraft.

An expanded time scale plot of the magnitude and three components of the magnetic field for the time interval indicated by A in Figure 1 is presented in Figure 2. As observed by Explorer 33, the time required for the direction of the field to change is less than 10.2 seconds. This is the time interval between two successive measurements of the magnetic field. However, when observed by Explorer 35 the time interval is 56.2 seconds with a clearly defined minimum in the magnetic field associated with the field reversal direction. We do not believe that a variable orientation of the discontinuity surface or a variation of its time profile in different places can explain all aspects of the observations. Most important is the existence of a significant anomaly in the X_{SSE} component of the field corresponding to the field reversal and field magnitude minimum.

We interpret this dilation of the discontinuity time profile to be due to the time required for the magnetic field change to diffuse through the interior of the moon. The time constant for a conducting sphere of radius R is given by $\tau = \mu\sigma R^2/\pi^2$ where μ = magnetic permeability, σ = electrical conductivity. The time scale of 56 seconds establishes the "Cowling" diffusion time for the lunar body as less than $56 / 3 \doteq 19$ seconds. Assuming a homogeneous conducting interior of radius R_M, then this implies an upper limit to the electrical conductivity of the lunar interior of $5 \times 10^{-5}\ (\Omega\text{-m})^{-1}$.

3.0 Interpretation

A study of various models of the electrical conductivity structure of the moon has recently been conducted (3). A summary of the results for different ages of a moon assumed to have a composition similar to olivine is shown in Figure 3. Here the electrical conductivity profile is seen to be a very sensitive function of the age assumed for the lunar body. The effective "Cowling" time constant for a homogeneous moon is also shown in Figure 3, assuming $R = R_M$.

It is clear from these curves that the assumption of a homogeneous electrically conducting moon cannot be justified. It will be assumed that the moon can be approximated by a two layer sphere with a conducting interior of radius $R=0.8\ R_M = 1426$ km and a relatively poorly conducting insulating layer of thickness approximately 400 km. The Cowling time constant of the interior is a sensitive function of the assumed radius so that lowering it to $0.8\ R_M$ will raise the electrical conductivity by a factor of $(0.8)^{-2}$. Thus it is concluded that the electrical conductivity of the interior of the moon is less than $8 \times 10^{-5}\ (\Omega\text{-m})^{-1}$ and this is seen to be between models A and B.

The electrical conductivity of silicate materials is a very sensitive function of both temperature and pressure. However, the pressures in the interior of the moon are not sufficient to lead to significant effects. Thus the variation of electrical conductivity in the lunar interior will be primarily due to composition and temperature (4).

It has been assumed that Moon's electrical conductivity can be represented by a silicate with approximately an olivine composition (3). The models which have been computed in Figure 3 are derived from a relationship between electrical conductivity and temperature. The temperature has been determined on the assumption that the moon has a typically chondritic meteorite radiogenic heat source composition.

In Figure 4 are summarized theoretical computations of the internal temperatures of the moon (3). The alphabetical notation on the curves corresponds to the electrical conductivity curves shown in Figure 3. Since the electrical conductivity inferred from the measurements of the discontinuities propagating past the moon is less than 10^{-4} mhos/meter, we infer that these measurements indicate that the models A and B are more favored versions than model C (both with and without melting). The latter both lead to very high electrical conductivities within the lunar interior, up to 10^{-2} $(\Omega\text{-m})^{-1}$ and time constants much longer than 100 seconds. The interior temperature for model A is approximately 1000°K while that for B is 2100°K. We infer from these measurements that the interior of the moon is relatively cool when compared to the much higher temperatures possible for model C. This means a temperature of approximately 1200°K using the conductivity of $8\text{x}10^{-5}(\Omega\text{-m})^{-1}$. Thus a model of the thermal history of Moon must be able to account for these relatively low temperatures and only a young Moon or an old but differentiated Moon has these properties.

This brief paper summarizes the experimental evidence from the NASA-Goddard Space Flight Center magnetic field experiment on Explorer 35 and its data relative to the problem of the interior state of the moon. A more expanded version including a discussion of the transparency of the moon to magnetic fluctuations in the interplanetary medium is in preparation.

REFERENCES

1. Behannon, K. W., Intrinsic Magnetic Properties of the Lunar Body, J. Geophys. Res., 73, 7257 (1968).
2. Burlaga, L. F., Micro-scale Structures in the Interplanetary Medium, Solar Physics, 4, 79, (1968).
3. England, A. W., Gene Simmons and D. Strangway, Electrical Conductivity of the Moon, J. Geophys. Res., 73, 3219, (1968).
4. Hamilton, R. M., Temperature Variation at Constant Pressures of the Electrical Conductivity of Periclase and Olivine, J. Geophys. Res., 70, 5679 (1965).
5. Hollweg, Joseph V., Interaction of the Solar Wind with the Moon and Formation of a Lunar Limb Shock Wave, J. Geophys. Res., 73, 7269, (1968).
6. Johnson, F. and J. E. Midgley, Note on the Lunar Magnetosphere. J. Geophys. Res., 73, 1523, (1968).
7. Ness, Norman F., Lunar Explorer 35, NASA-GSFC Preprint X-616-68-166, (1968). To be published in Proceedings XIth COSPAR (1969).
8. Tozer, D. C. and J. Wilson, The Electrical Conductivity of the Moon's Interior, Proc. Roy. Soc., A. 296, 320 (1967).

FIGURE CAPTIONS

Figure 1 Simultaneous interplanetary magnetic field measurements by Explorers 33 and 35 in February 1968. At this time Explorer 33 was located at (37.3, -56.3, -23.3) and Explorer 35 at (59.5, -8.4, -4.0) in geocentric solar ecliptic coordinates (units are Earth Radii- 6378.1 km). Discontinuity occurs midway during time interval A.

Figure 2 Detailed simultaneous component measurements of convection of interplanetary magnetic field discontinuity at Explorer 35 Sequence No. 249791 past moon on February 27, 1968.

Figure 3 Electrical conductivity as a function of depth for different ages for olivine Model of moon (adapted from (5)).

Figure 4 Temperature as a function of depth for different ages of moon assuming a radiogenic composition similar to chondritic meteorites. D is Albite solidus, E is locus of equal contribution by ionic and electronic processes, F is diopside solidus (5).

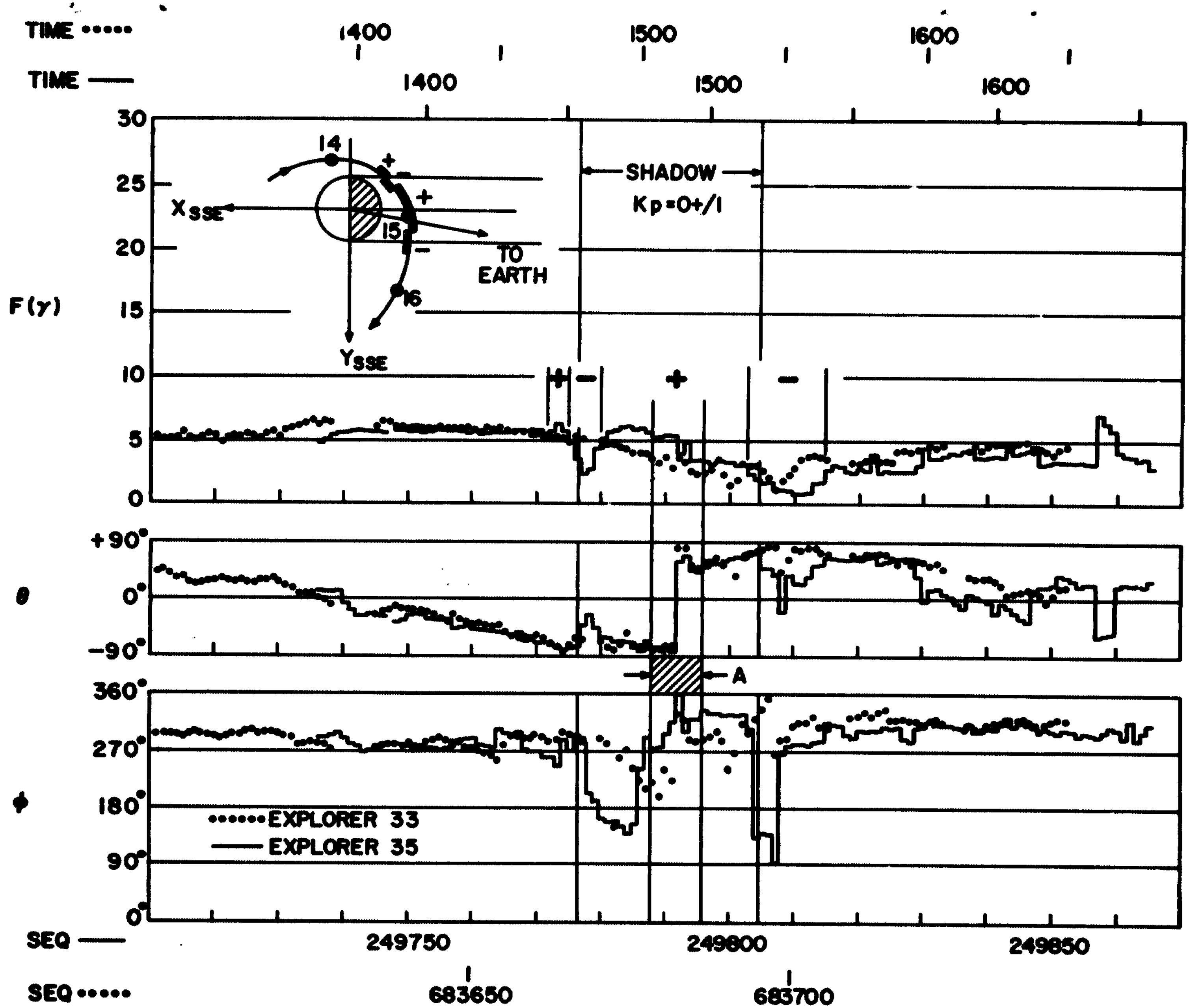

27 FEBRUARY 1968

FIGURE 1

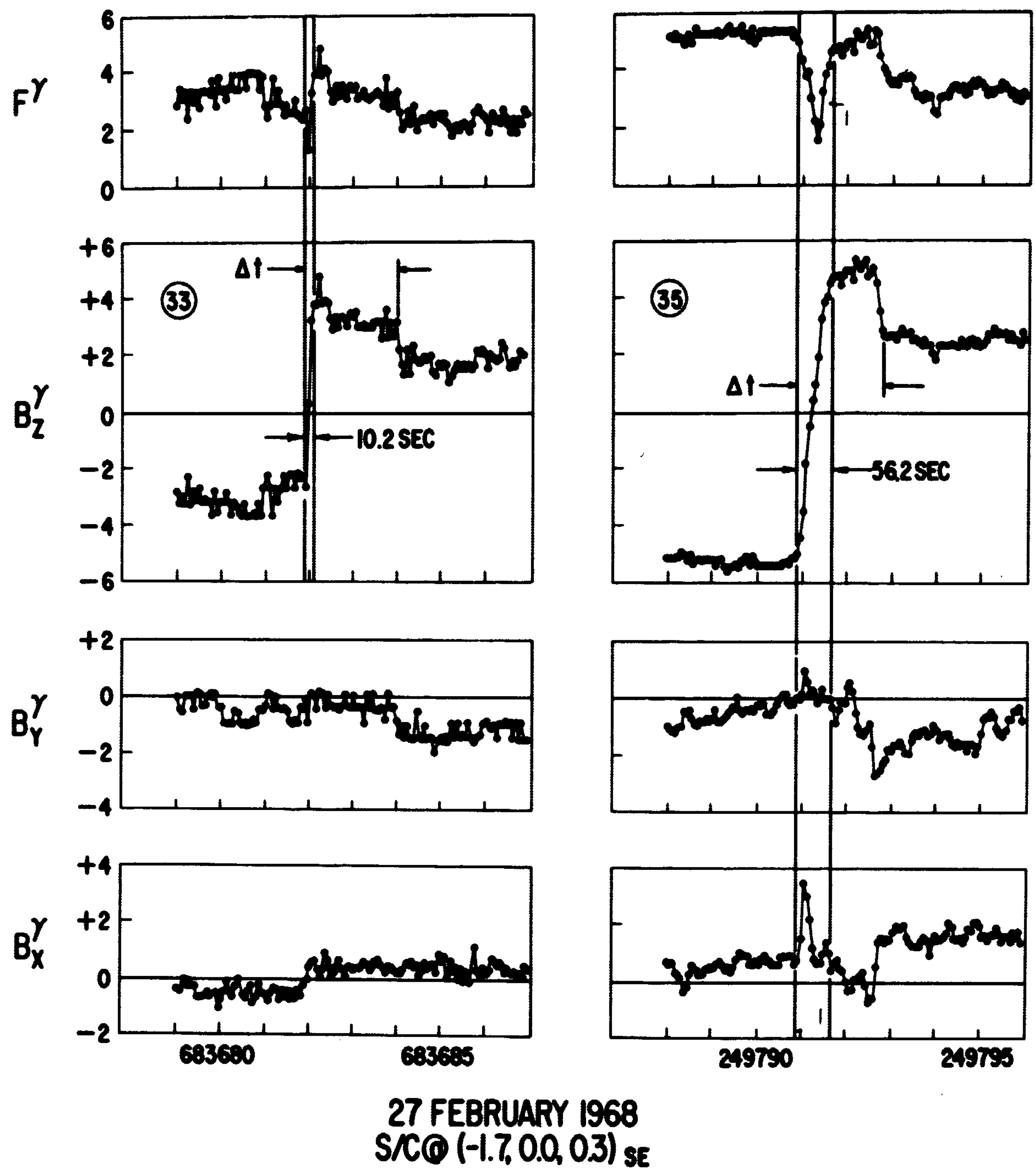

F^γ
B_Z^γ
B_Y^γ
B_X^γ
33
35
Δt
10.2 SEC
56.2 SEC
683680
683685
249790
249795
27 FEBRUARY 1968
S/C@ (-1.7, 0.0, 0.3) SE

FIGURE 2

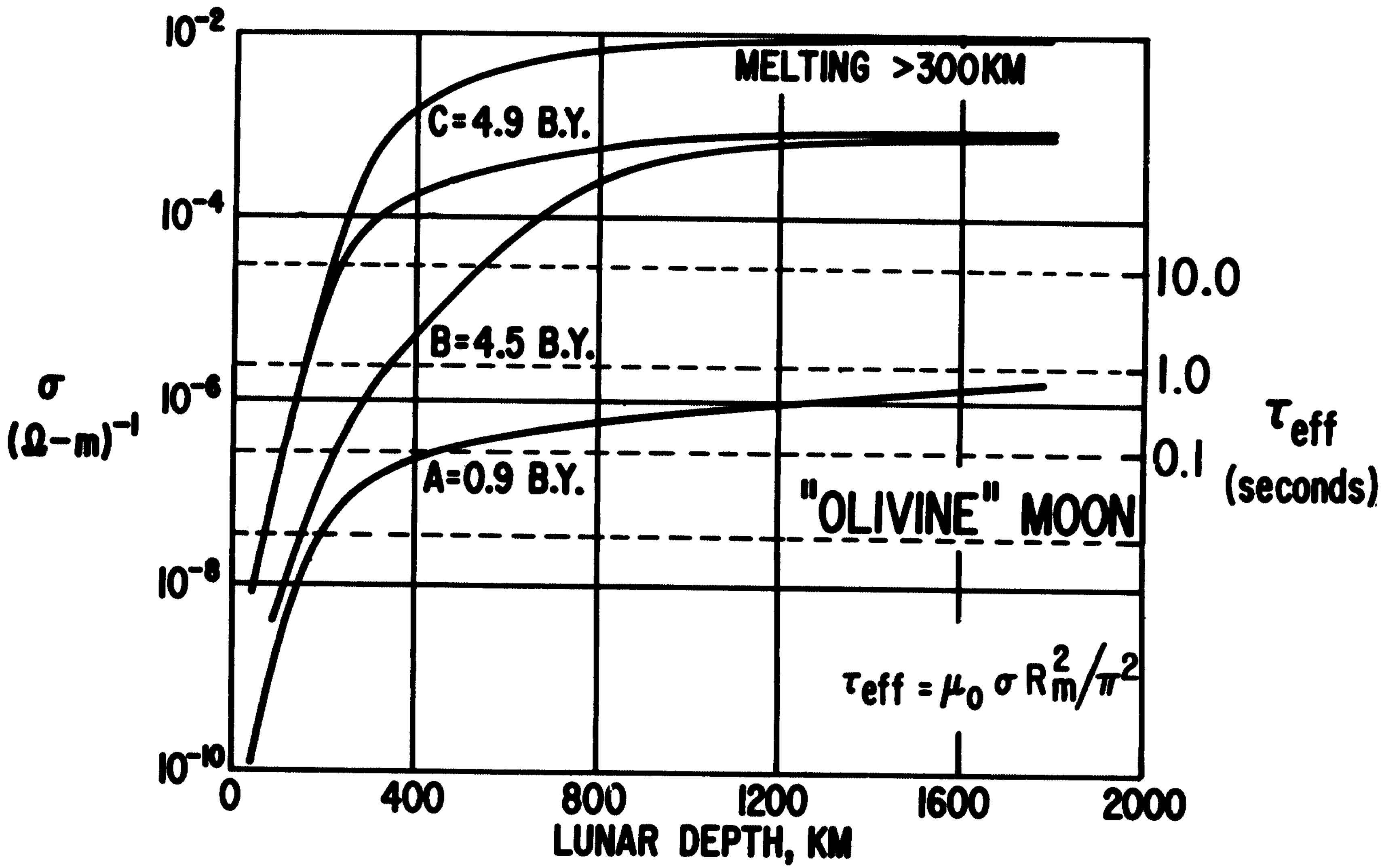

MELTING >300KM
C=4.9 B.Y.
B=4.5 B.Y.
A=0.9 B.Y.
"OLIVINE" MOON
$\tau_{eff} = \mu_0 \sigma R_m^2/\pi^2$
σ $(\Omega-m)^{-1}$
10^{-2}
10^{-4}
10^{-6}
10^{-8}
10^{-10}
0
400
800
1200
1600
2000
LUNAR DEPTH, KM
10.0
1.0
0.1
τ_{eff} (seconds)

FIGURE 3

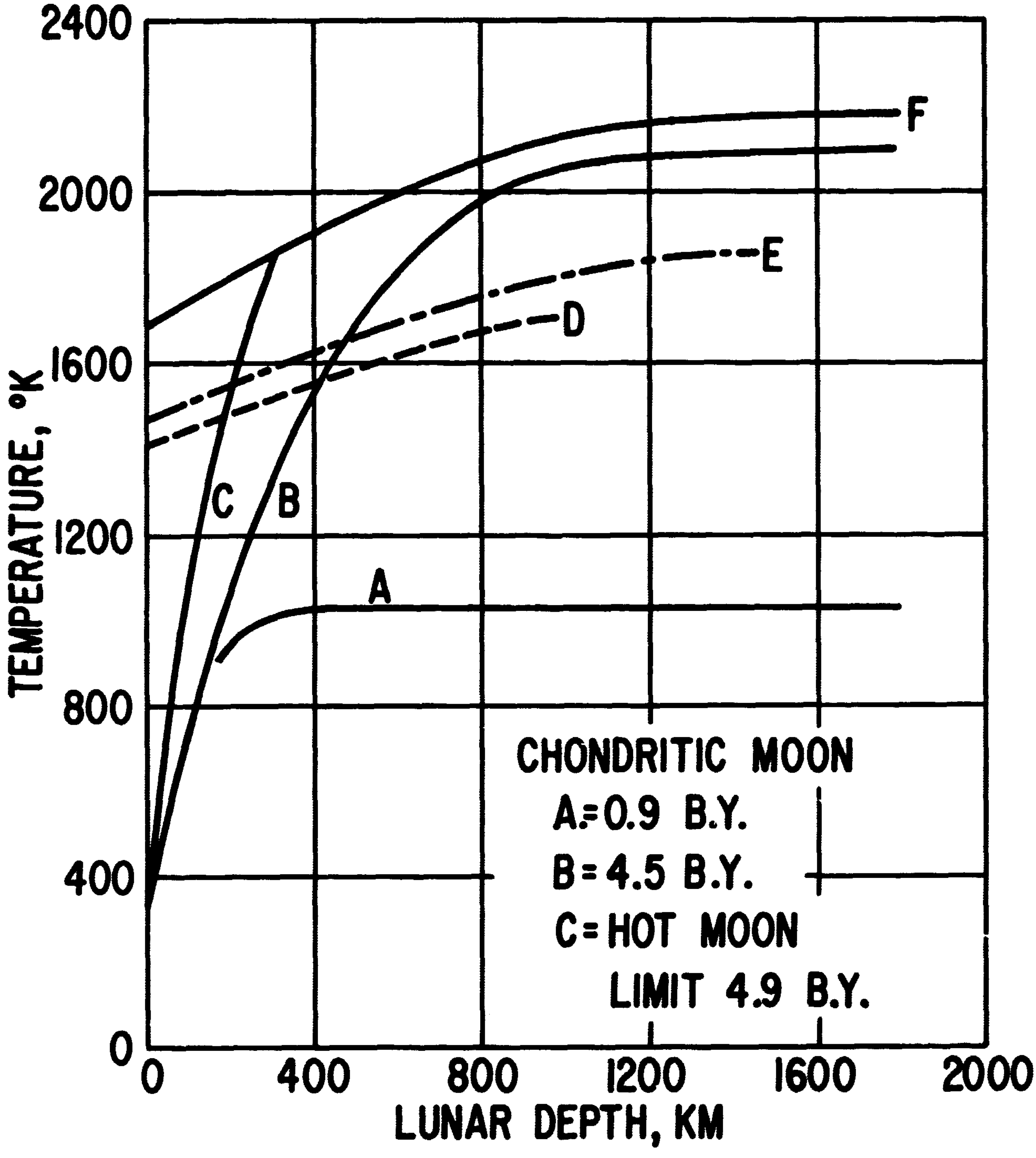

2400
2000
1600
1200
800
400
0
TEMPERATURE, °K
0
400
800
1200
1600
2000
LUNAR DEPTH, KM
F
E
D
C
B
A
CHONDRITIC MOON
A=0.9 B.Y.
B=4.5 B.Y.
C=HOT MOON
LIMIT 4.9 B.Y.

FIGURE 4